J. Phys. B: At. Mol. Phys. **17** (1984) 2841–2850. Printed in Great Britain

The doubly differential alignment parameter A_2 for L_3 subshell ionisation by light-ion impact

R Spies†, H Böckl†, F Bell† and D H Jakubassa-Amundsen‡

† Physics Section, University of Munich, D-8046 Garching, Federal Republic of Germany
‡ Physics Department, Technical University of Munich, D-8046 Garching, Federal Republic of Germany

Received 5 January 1984, in final form 28 February 1984

Abstract. The alignment parameter A_2 for electron emission from the L_3 subshell, doubly differential in energy and angle, has been calculated with the plane-wave Born approximation. Both the alignment of target atoms and projectile ions will be discussed.

1. Introduction

In recent years alignment studies of inner shells by light-ion impact have attracted both experimental and theoretical interest (Rösel *et al* 1982, Berezhko and Kabachnik 1977, Sizov and Kabachnik 1980, Kamiya *et al* 1979, Pálinkás *et al* 1980). While in the past the main work has been concentrated on total cross section measurements (Jitschin *et al* 1982, Schöler and Bell 1978, Kabachnik *et al* 1980, Wigger *et al* 1981) the interest has now turned to differential cross section measurements which provide an impact-parameter-dependent alignment parameter A_2 (Konrad *et al* 1984). Kocbach *et al* (1983) have published an extensive study of the impact parameter dependence of $A_2(b)$ within the framework of the non-relativistic semiclassical approximation (SCA). An important result of these calculations was that one can obtain more detailed information about the collision dynamics from $A_2(b)$ than from the non-coincident measurements of A_2: whereas the alignment obtained from total cross sections is vanishingly small for $\kappa^2 = (v_p/v_{or})^2 > 0.3$ (v_p is the projectile velocity and $v_{or} = Z_T/2$ is the orbital velocity of the L_3-shell electron) $A_2(b)$ can still obtain large values, negative at small impact parameters b and positive at large b values. Thus integration over b yields nearly zero alignment.

An alternative way to get insight into the collision dynamics and provide a sensitive test of theoretical models, is the investigation of the doubly differential cross section with respect to the energy and direction of the emitted electron. It is the aim of this paper to give information on the alignment parameter A_2 as a function of both energy and direction of the ejected electron. In § 2, the PWBA theory is sketched, and §§ 3 and 4 give a discussion of the target and projectile alignment, respectively. In § 5, the validity of the PWBA is investigated by including the coupling between the magnetic substates. Atomic units ($\hbar = m = e = 1$) are used throughout.

0022-3700/84/142841+10$02.25

2. The model

For high collision velocities v_p and small projectile charges Z_p the doubly differential cross section for target electron emission into the state ψ_f can be calculated in the plane-wave Born approximation (PWBA):

$$\frac{d^2\sigma}{dE\, d\Omega} = \frac{4Z_p^2}{v_p^2} u \int_{q_{min}}^{\infty} \frac{dq}{q^3} \int_0^{2\pi} d\varphi_q |\langle \psi_f | \exp(i\boldsymbol{q}\cdot\boldsymbol{r}) | \psi_i \rangle|^2 \tag{1}$$

with $q_{min} = (E - E_i)/v_p$ and E_i the energy of the initial electronic state ψ_i. The electron is ejected with velocity u, i.e. energy $E = u^2/2$ into the solid angle $d\Omega$. When hydrogenic non-relativistic wavefunctions are used, the ionisation matrix element can be calculated analytically for any initial state by means of partial derivatives (with respect to the target charge Z_T or the momentum transfer $\boldsymbol{q}$) of the 1s ionisation matrix element given by McDowell and Coleman (1970). The quantisation axis is chosen parallel to the beam direction $\hat{\boldsymbol{v}}_p$. Even then, the integral over the azimuthal angle φ_q can be done analytically, whereas the integral over q is calculated numerically. In the case of projectile ionisation (1) can be used with the interchange of Z_p and Z_T, but now instead of u, E and $d\Omega$ the velocity v, energy and solid angle in the projectile rest frame enter, and a transformation to the target (i.e. laboratory) frame become necessary.

The alignment parameter A_2 is defined as (Fano and Macek 1973)

$$A_2(u_\parallel, u_\perp) = \frac{(d^2\sigma/dE\, d\Omega)_{m=1} - (d^2\sigma/dE\, d\Omega)_{m=0}}{2(d^2\sigma/dE\, d\Omega)_{m=1} + (d^2\sigma/dE\, d\Omega)_{m=0}} \tag{2}$$

where $(d^2\sigma/dE\, d\Omega)_{m=0,1}$ is the doubly differential cross section for the ionisation of the 2p, $m = 0$ and 2p, $m = 1$ states, respectively, and $u_\parallel$ and $u_\perp$ are the components of the electron velocity parallel and perpendicular to the beam direction. Experimentally, the alignment could be found by a coincidence between a delta electron with energy E emitted at angle θ to the beam direction and a photon or an Auger electron which is characteristic of the L_3 subshell. It should be emphasised that the measurement of A_2 demands azimuthal symmetry of the δ electron spectrometer.

3. Target alignment

It can be shown that for hydrogenic wavefunctions and a pure Coulomb interaction between the projectile and the bound electron the alignment parameter A_2 scales with $\xi = u/v_{or}$ for constant κ. Figure 1 parts (*a*)–(*c*) shows contour lines of A_2 for $\kappa = 0.2$, 0.4 and 4. It is evident that at small u/v_{or} the alignment parameter changes dramatically with κ. In figure 2 A_2 is plotted for $u_\perp = 0$ as a function of $u_\parallel/v_{or}$ and κ^2. At small $(u_\parallel/v_{or})$ values the alignment is negative at low velocities v_p but increases to small positive values with increasing projectile velocity v_p. If it is remembered that the total cross section is mainly determined by integration over small (u/v_{or}) values the behaviour of the total alignment is understood: whereas at low velocities v_p the differential alignment is negative for every ejection direction, at high velocities negative alignment in forward direction is mainly compensated by positive alignment at about 90° ejection angle.

The ring-shaped pattern of figure 1(*c*) reflects the binary encounter peak at $u = 2v_p \cos\theta$. There, the alignment is positive and reaches its maximum possible value $A_2 = +0.5$. It has been demonstrated that at large projectile velocities ($\kappa > 1$) the doubly

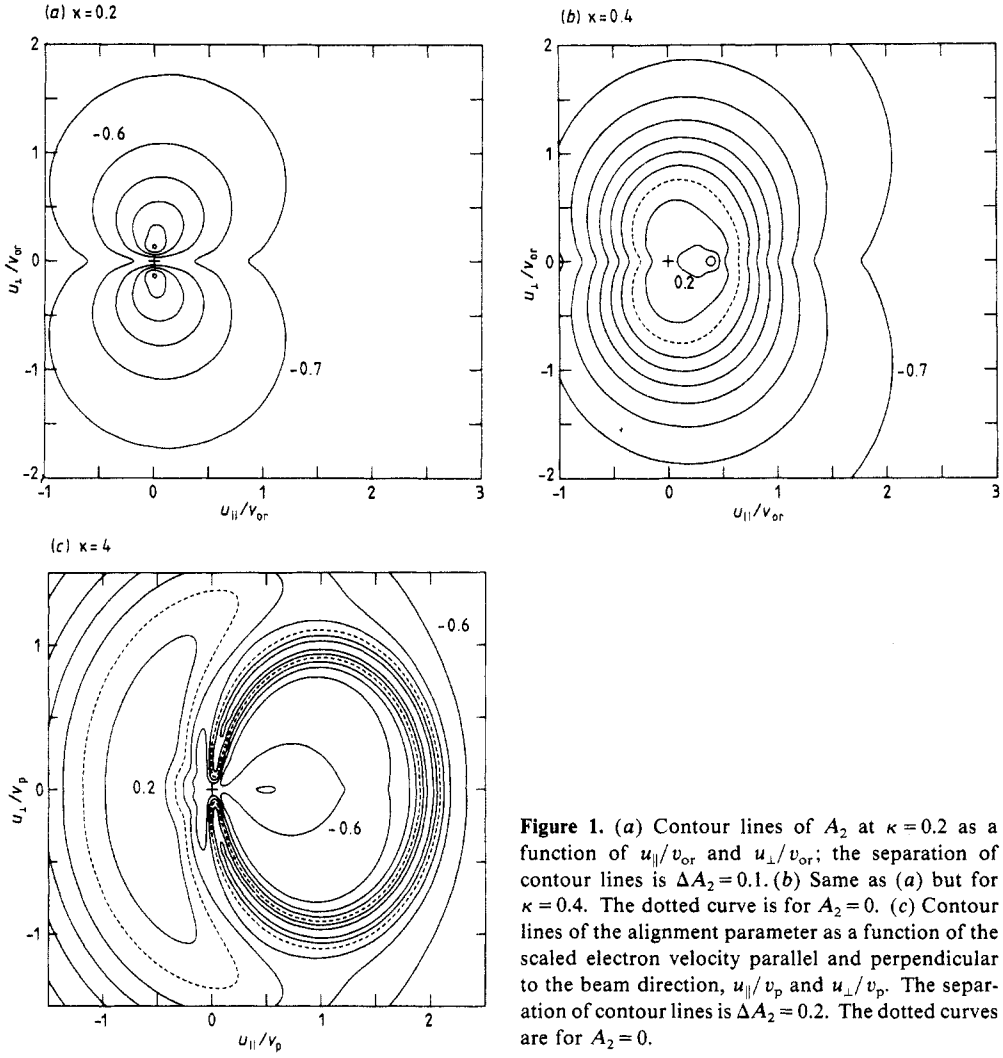

Figure 1. (*a*) Contour lines of A_2 at $\kappa = 0.2$ as a function of $u_{\|}/v_{or}$ and $u_{\perp}/v_{or}$; the separation of contour lines is $\Delta A_2 = 0.1$. (*b*) Same as (*a*) but for $\kappa = 0.4$. The dotted curve is for $A_2 = 0$. (*c*) Contour lines of the alignment parameter as a function of the scaled electron velocity parallel and perpendicular to the beam direction, $u_{\|}/v_p$ and $u_{\perp}/v_p$. The separation of contour lines is $\Delta A_2 = 0.2$. The dotted curves are for $A_2 = 0$.

differential cross section can be factorised (Bell *et al* 1983)

$$\frac{d^2\sigma}{dE\, d\Omega} = \frac{1}{2v_p}\left(\frac{d\sigma}{d\Omega}\right)_R J(p_z) \tag{3}$$

where $(d\sigma/d\Omega)_R$ is the Rutherford cross section for the scattering of a free electron into $d\Omega$ by a projectile of velocity v_p and $J(p_z)$ is the Compton profile of the shell under consideration. The intrinsic momentum p_z is fixed by energy and momentum conservation: $p_z v_p = u v_p \cos\theta - \frac{1}{2}u^2$. From hydrogenic wavefunctions Compton profiles J_0 and J_1 for $2p_0$ and $2p_1$ substates are easily derived (per electron):

$$J_0 = \frac{2^7 (p_z/p_{or})^2}{5\pi p_{or}[1+(p_z/p_{or})^2]^5}$$
$$J_1 = \frac{2^4}{5\pi p_{or}[1+(p_z/p_{or})^2]^4}. \tag{4}$$

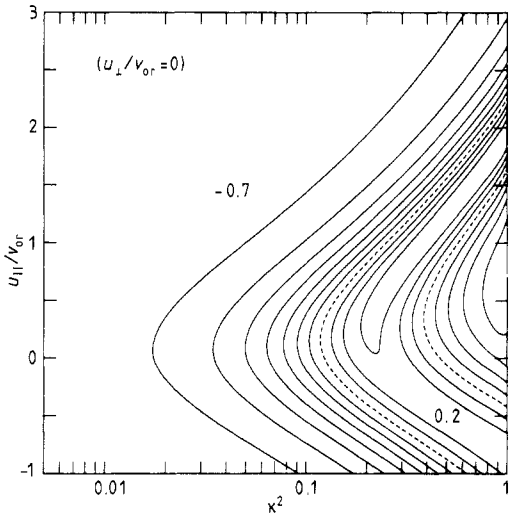

Figure 2. Contour lines of A_2 at $u_\perp/v_{or}=0$ as a function of $u_\parallel/v_{or}$ and $\kappa^2=(v_p/v_{or})^2$. $\Delta A_2=0.1$. The broken curves indicate $A_2=0$.

p_{or} is the orbital momentum of the target atom ($p_{or}=v_{or}$ in au). Thus, the alignment in the binary encounter peak region is given by

$$A_2=\frac{4\kappa^2-7(2\xi\kappa\cos\theta-\xi^2)^2}{8\kappa^2+10(2\xi\kappa\cos\theta-\xi^2)^2}. \tag{5}$$

From equations (3) and (4) it is evident that $(d^2\sigma/dE\,d\Omega)_{m=1}$ has a *maximum* at the position of the binary encounter peak but $(d^2\sigma/dE\,d\Omega)_{m=0}$ has a *minimum*. This peak inversion for $m=0$ is accompanied by two separated peaks at (see also figure 5)

$$\xi^2\simeq 4\kappa^2\cos^2\theta\pm 2\kappa \tag{6}$$

where $\kappa\cos\theta\gg 1$ has been used.

The peak inversion at the position of the binary encounter peak is a direct consequence of the nodal plane of the $2p_0$ wavefunction perpendicular to the beam direction. It is the analogue of the very recently found cusp inversion for projectile electrons emitted in the forward direction (Burgdörfer 1983, Burgdörfer *et al* 1983).

4. Projectile alignment

Figure 1(*c*) especially reveals that the alignment changes rather quickly both with ejection velocity u and ejection angle θ in the neighbourhood of the origin at $u=0$. This demonstrates the sensitivity of the alignment for the collision dynamics. It might be that this region is accessible to the experiment if electrons from the cusp-shaped forward peak in ion–atom collisions are measured (Sellin *et al* 1982). For dressed ions a constituent part of the cusp electrons might result from 2p ionisation of the projectile. Thus measuring for example the angular anisotropy of the L_l-radiation of a projectile in coincidence with electrons of the cusp means to move a disc with extension $u/v_p=2\theta_0$ across the origin of figure 1(*c*) (θ_0 is the electron spectrometer acceptance angle). In order to investigate the alignment in this region more extensively, we have extended

the theory of Day (1980, 1981) for the cusp shape from 1s ionisation to $2p_{0,1}$ electron loss to the continuum (ELC). It can be shown quite generally, that the Galilean-invariant doubly differential cross section $d\sigma/dv$ for ELC from $2p_{0,1}$ states can be written (Böckl *et al* 1984)

$$\lim_{v\to 0}\left(v\frac{d\sigma}{dv}\right)_m = \sigma_{0m}(1 + a_{2m}P_2(\cos\theta) + a_{4m}P_4(\cos\theta)). \tag{7}$$

Here, v is the electron velocity in the projectile frame and θ the electron emission angle relative to the projectile velocity $-v_p$. The index $m = 0, 1$ characterises the magnetic substates of $|2p\rangle$, where the quantisation axis is taken parallel to the beam direction. The coefficients a_{im} of the Legendre polynomials P_i depend on κ only. Transforming equation (7) to the laboratory frame and integrating over the angular acceptance θ_0 of the electron spectrometer (neglecting finite-energy resolution) yields the singly differential cross section for ELC

$$\left(\frac{d\sigma}{dE}\right)_m = 2\pi\left(\frac{u}{v_p}\right)^{1/2}\theta_0\sigma_{0m}\left[(A_m + B_m - C_m)|\eta| - (1+\eta^2)^{1/2}\left(\frac{A_m\eta^4}{(1+\eta^2)^2} + \frac{B_m\eta^2}{1+\eta^2} - C_m\right)\right] \tag{8}$$

with

$$\begin{aligned} A_m &= 35a_{4m}/24 \qquad B_m = 3a_{2m}/2 - 15a_{4m}/4 \\ C_m &= 1 - a_{2m}/2 + 3a_{4m}/8 \\ \eta &= (u - v_p)/(uv_p)^{1/2}\theta_0. \end{aligned} \tag{9}$$

The four coefficients a_{im} and the ratio $\gamma = \sigma_{01}/\sigma_{00}$ are functions of κ only, as displayed in figure 3. The resulting alignment parameter $A_2(\eta, \kappa)$ depends also only on κ if an unscreened Coulomb interaction between the projectile electron and the target atom is assumed. Figure 4 shows A_2 as a function of the scaled electron velocity difference η for selected values of κ. It is seen that for $\kappa < 1$ the alignment parameter A_2 is essentially independent of η. Comparison with figure 3 reveals that this results from the vanishing of the angular anisotropy parameters a_{im}. In this regime A_2 is determined by the cross section ratio γ only: $A_2 \simeq (\gamma - 1)/(2\gamma + 1)$. For $\kappa > 1$ the alignment parameter shows a cusp-like behaviour. This alignment cusp is determined by the angular anisotropy only in contrast to the electron *yield* cusp which is given in essence by the isotropic part of the cross section (Day 1980, 1981). For $\kappa \gg 1$ the limiting values of a_{im}—which are reached logarithmically only—are: $a_{20} = \frac{5}{7}$, $a_{40} = -\frac{12}{7}$, $a_{21} = -\frac{120}{91}$ and $a_{41} = \frac{64}{91}$. From that one derives that for $m = 0$ the doubly differential cross section for low electron velocities has a maximum at $\theta = \pm 45°$. For $m = 1$ there exists a small emission maximum at $\theta = 0$ and a much bigger one at $\theta = \pm 90°$. Thus, both states exhibit typical quadrupole emission patterns. Figure 5 shows a two-dimensional plot of local maxima of the doubly differential cross section for the two magnetic substates $m = 0$ (full curve) and $|m| = 1$ (broken curve). If a disc-like detection volume of an electron spectrometer is moved across the origin at $v = 0$, the $2p_0$ substate shows an inverted cusp-like electron yield whereas $2p_1$ has an ordinary cusp yield. This cusp inversion has recently also been recognised by Burgdörfer (1983). Since the cross section ratio γ is approximately unity for $\kappa > 1$ it follows from these considerations that the alignment parameter A_2 has a cusp-like behaviour, too. In the high velocity

limit the alignment even reaches its maximum possible value for small values of η:

$$A_2 \simeq \frac{1}{2} - \frac{3(A_0 + B_0)}{4\gamma C_1}|\eta| \qquad \kappa \gg 1. \tag{10}$$

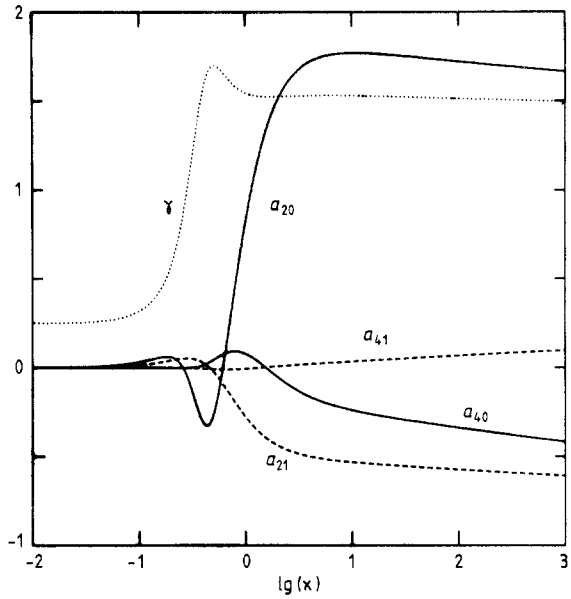

Figure 3. The angular anisotropy parameters a_{lm} and the cross section ratio γ as a function of κ.

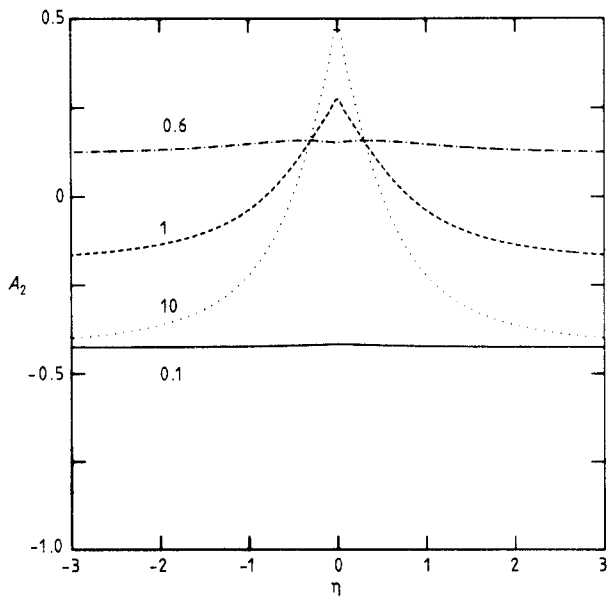

Figure 4. Projectile alignment A_2 as a function of the electron velocity η. This alignment is expected at the electron yield cusp near $u = v_p$. The numbers on the curves are the corresponding values of κ.

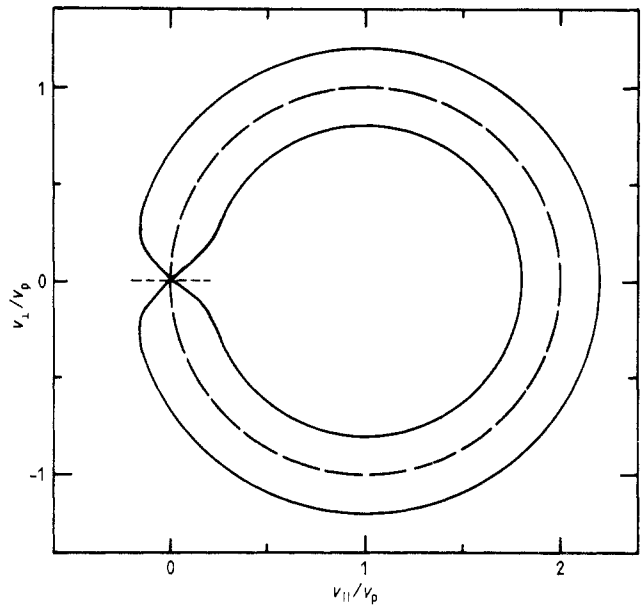

Figure 5. The positions of local maxima for the doubly differential cross sections $(d^2\sigma/dE\, d\Omega)_m$: $m=0$ (full curve), $m=1$ (dotted curve). $\kappa=2.8$.

Equation (10) reveals that the alignment parameter A_2 shows a cusp-like behaviour if the prefactor of $|\eta|$ is positive. Since $C_1 \geqslant 0$ for all κ the sufficient condition for an alignment cusp is $A_0+B_0 \geqslant 0$. Inspection of equation (8) shows that this condition demands simultaneously the inversion of the $2p_0$ electron yield cusp ($C_0 \to 0$ for $\kappa \gg 1$). Thus the alignment cusp seems to be an experimentally accessible signature—and maybe the only one—of the $2p_0$ electron yield cusp (Burgdörfer 1983).

5. Validity of the PWBA

In order to discuss the limitations of the formula (1) we use the equivalent semiclassical description. We also restrict ourselves to target ionisation.

At small projectile velocities a straight-line internuclear trajectory will no longer be appropriate, even for asymmetric collision systems. The Coulomb deflection can be estimated from the correction factor $\exp(-\pi d q_{\min})$ where d is half the distance of closest approach in a head-on collision (Bang and Hansteen 1959). For the collision system $p \to Ne$, Coulomb deflection becomes important for $\kappa < 0.2$. However, as the $m=0$ and $m=1$ subshell cross sections will be reduced in a similar way, we do not expect a large change of the alignment.

More crucial is the breakdown of the first-order Born approximation at the lower collision velocities. As the 2p, $m=0$ and 2p, $m=1$ states are degenerate, there is a strong coupling between these states during or after the ionisation process such that their relative occupation number and thus the alignment will be changed. While this change of A_2 may be averaged out if only total cross sections are considered, it should be visible in the doubly differential cross sections studied here. The inclusion of

higher-order Born terms in the calculation of the alignment has been discussed by Sarkadi and Mukoyama (1981) in a simplified treatment where the first-order ionisation cross sections are multiplied by the corresponding probabilities for intrashell transitions. This model thereby neglects interference effects between the ionisation and the coupling process which are important if a definite final state of the electron is observed.

In order to estimate the effect on A_2, we have taken the coupling between the $m=0$ and $m=1$ states fully into account, while treating the excitation to the continuum in perturbation theory. The amplitudes a_m for finding a vacancy in the 2p,m states with energy E_i are obtained from the differential equations

$$\begin{aligned} \dot{a}_0 &= -\mathrm{i}a_0E_i - \mathrm{i}a_0V_{00} - 2\mathrm{i}a_1V_{10} - \mathrm{i}V_{0f}\exp(-\mathrm{i}Et) \\ \dot{a}_1 &= -\mathrm{i}a_0V_{10} - \mathrm{i}a_1(V_{11}-V_{1-1}) - \mathrm{i}a_1E_i - \mathrm{i}V_{1f}\exp(-\mathrm{i}Et) \\ V_{mm'} &= \left\langle \psi_{2\mathrm{p}m} \left| \frac{-Z_\mathrm{p}}{|\boldsymbol{R}-\boldsymbol{r}|} \right| \psi_{2\mathrm{p}m'} \right\rangle \end{aligned} \tag{11}$$

where $a_{-1}=-a_1$ has been used and in the source terms the matrix elements are formed with the continuum state ψ_f of energy E. The internuclear trajectory $\boldsymbol{R}(t)$ is taken as a straight line with impact parameter $\boldsymbol{b}$. Formula (1) is then replaced by

$$\left(\frac{\mathrm{d}^2\sigma}{\mathrm{d}E\,\mathrm{d}\Omega}\right)_m = u\int \mathrm{d}^2\boldsymbol{b}\,|a_m(t=+\infty)|^2. \tag{12}$$

Numerical inspection of (11) reveals that the change of $a_m(t)$ from the subshell coupling (i.e. from $V_{mm'}$) alone extends over a time range from t_0 (<0) to t_1 which depends only weakly on v_p for a given collision system. On the other hand, the change of $a_m(t)$ from the inhomogenity V_{mf} proceeds over a time range $\Delta t \gg t_1 - t_0$ which is strongly velocity dependent because of the large momentum transfer. Instead of solving (11) with the initial conditions $a_m(t_i)=0$ ($t_i \ll t_0$) we therefore started at t_0 and equated $a_m(t_0)$ to the (first order) ionisation amplitudes at t_0. This corresponds to setting $V_{mm'}=0$ for $t<t_0$. Similarly we took $V_{mm'}=0$ for $t>t_1$ and added to $a_m(t_1)$ only the missing part of the ionisation amplitudes. This procedure speeds up the convergence considerably.

From equation (11) it becomes obvious that the scaling properties of A_2 with only ξ and κ are lost, as an additional dependence on Z_p emerges which increases the influence of the subshell coupling for growing Z_p. Figure 6 shows the alignment for protons colliding with Ne as a function of $\kappa = v_\mathrm{p}/v_\mathrm{or}$ at a fixed electron velocity $u_\parallel/v_\mathrm{or}=0.4$ and $u_\perp=0$. For $v_\mathrm{p}\sim 1(\kappa\sim 0.2)$ interference effects are largest because the impact parameter (or time) where ionisation predominantly occurs, is the same as that for which the subshell coupling mainly takes place. However, the deviations from the first Born approximation extend to rather large κ which is based on the fact that the amplitudes a_m around $t=0$ are considerably larger than at $t\to\infty$ such that small changes from the coupling produce a big effect on the asymptotic probabilities. When studying the dependence of A_2 on the electron velocity at fixed collision energy, the subshell coupling gives similar results to the Born theory for $u/v_\mathrm{or}\leqslant 0.5$. At high-$u$ velocities where the momentum transfer to the electron is large, the coupling mainly takes place on the outgoing part of the collision. This leads predominantly to a refilling of the $2\mathrm{p}_0$ state and thus to an increase of the alignment even for $\kappa\sim 0.4$. The rather large change of A_2 would be completely underestimated by a mere multiplication of probabilities following the Sarkadi and Mukoyama (1981) prescription.

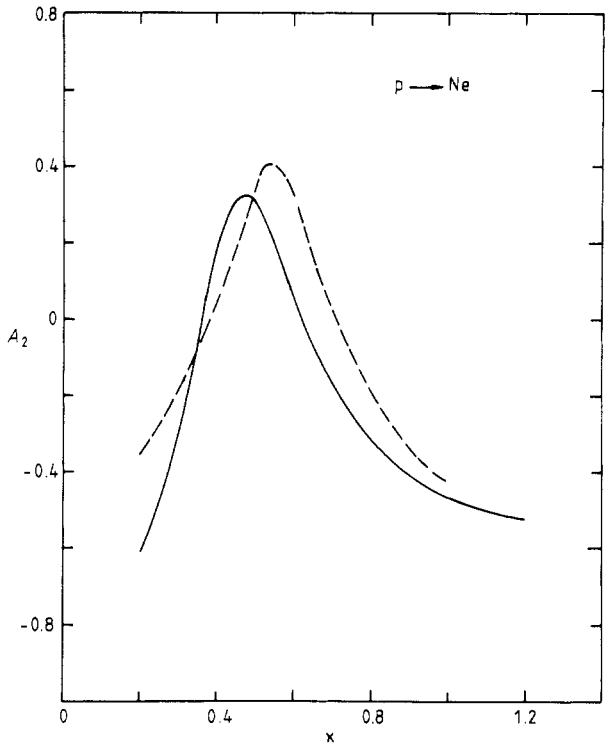

Figure 6. Alignment A_2 in p→ Ne collisions as a function of the scaled projectile velocity. The electron velocity is taken parallel to the beam axis with $u_{\parallel}/v_{or} = 0.4$. Full curves are the first Born results, broken curves the coupling result from (12).

6. Conclusion

We have calculated the alignment of the 2p shell within the framework of the PWBA using hydrogenic wavefunctions. An improvement would be the use of Hartree–Fock wavefunctions for both the initial and final state. While such a calculation would not change the cross sections and thus the alignment at the binary encounter peak and even larger electron velocities we expect deviations at small (u/v_{or}) values. Although quantitative differences from the results described above might exist, qualitatively the behaviour of A_2 for small electron velocities remains correct. This, at least, is an experience from the alignment obtained by total cross sections (Sizov and Kabachnik 1980, Kabachnik *et al* 1980).

In the case of projectile alignment one might argue additionally that the target–projectile interaction is not pure Coulombic but screened. However, the introduction of an exponential screening changes the angular anisotropy parameters a_{im} only slightly (Böckl *et al* 1984).

When the PWBA is modified to include subshell coupling of the 2p, m states the alignment is affected for the smaller values of the projectile velocity. However, the qualitative dependence of A_2 on v_p and the electron velocity u is retained, which means only a slight rescaling of the alignment patterns displayed in the figures.

Acknowledgment

This work has been partially supported by the Bundesministerium für Forschung und Technologie and by the GSI Darmstadt.

References

Bang J and Hansteen J M 1959 *K. Danske Vidensk. Selsk. Mat.-Fys. Meddr.* **31** No 13
Bell F, Böckl H, Wu M Z and Betz H D 1983 *J. Phys. B: At. Mol. Phys.* **16** 187–95
Berezhko E G and Kabachnik N M 1977 *J. Phys. B: At. Mol. Phys.* **10** 2467–77
Böckl H, Spies R, Bell F and Jahubassa-Amundsen D H 1984 *Phys. Rev.* A **29** 983–4
Burgdörfer J 1983 *Phys. Rev. Lett.* **51** 374–77
Burgdörfer J, Breinig M, Elston S B and Sellin I A 1983 *Phys. Rev.* A **28** 3277–90
Day M H 1980 *J. Phys. B: At. Mol. Phys.* **13** L65–8
—— 1981 *J. Phys. B: At. Mol. Phys.* **14** 231–42
Fano U and Macek J H 1973 *Rev. Mod. Phys.* **45** 553–73
Jitschin W, Kaschuba A, Kleinpoppen H and Lutz H O 1982 *Z. Phys.* A **304** 69–73
Kabachnik N M, Petukhov V P, Romanovskii E A and Sizov V V 1980 *Sov. Phys.–JETP* **51** 869–74
Kamiya M, Kinefuchi Y, Endo H, Kuwako A, Ishii K and Morita S 1979 *Phys. Rev.* A **20** 1820–7
Kocbach L, Hansteen J M and Gundersen R 1983 *Phys. Scr.* **27** 54–8
Konrad J, Schuch R, Hoffmann R and Schmidt-Böcking H 1984 *Phys. Rev. Lett.* **52** 188–91
McDowell M R C and Coleman J P 1970 *Introduction to the Theory of Ion–Atom Collisions* (Amsterdam: North-Holland) p 364
Pálinkás J, Sarkadi L and Schlenk B 1980 *J. Phys. B: At. Mol. Phys.* **13** 3829–34
Rösel F, Trautmann D and Baur G 1982 *Z. Phys.* A **304** 75–8
Sarkadi L and Mukoyama T 1981 *J. Phys. B: At. Mol. Phys.* **14** L255–60
Schöler A and Bell F 1978 *Z. Phys.* A **286** 163–8
Sellin I A, Breinig M, Brandt W and Laubert R 1982 *Nucl. Instrum. Meth.* **194** 395–404
Sizov V V and Kabachnik N M 1980 *J. Phys. B: At. Mol. Phys.* **13** 1601–10
Wigger J, Ost S, Brüssermann M and Cleff B 1981 *Phys. Lett.* **84**A 110–4